DER Analysis with Effective Load Carrying Capability for Enhanced Carbon-Aware Active Distribution System Resilience

Abdollah Younesi, *Student Member, IEEE,* Zongjie Wang, *Member, IEEE*, and Timothy M. Hansen, *Senior Member, IEEE*

***Abstract*—The resilience of active distribution systems against high-impact low-probability (HILP) events is a concern for distribution system operators (DSOs) and operators. In the short term, the optimal scheduling of distribution systems including various distributed energy resources (DERs) can improve the grid's resilience without much extra cost and time. Considering the reliable extra power that the DERs can supply, which is known as the DER's effective load-carrying capability (ELCC), this paper aims to integrate ELCC calculations into the general resilience-oriented distribution system scheduling methodology. In this way, the mesh view of the distribution system is first obtained to exactly calculate the location of the system components. Then, scenarios are generated based on the market characteristics and the HILP event features, such as location, type, and severity level. Finally, the proposed methodology is developed by integrating the generalized distribution system scheduling methodology with ELCC calculations considering uncertainties and carbon emissions. The proposed method is applied to an augmented IEEE 33-bus test system with DERs. Results show that the ELCC of DERs is a cost-effective method to improve distribution system resilience in the short term.**

***Index Terms*—Effective load-carrying capability, active distribution system, grid resilience, HILP events**

I. Introduction

Traditional distribution networks are gradually transforming into active distribution networks (ADNs) because of the integration of distributed energy resources (DERs) and smart switches, which present huge economic and environmental benefits [1]. In addition, integrating DERs into ADNs can improve the resilience of such systems against high-impact low-probability (HILP) events [2]. HILP events, such as severe natural disasters or cyber-attacks, present significant challenges to power systems. These rare but potent occurrences can lead to widespread outages, emphasizing the crucial importance of implementing robust resilience measures to safeguard the stability and functionality of energy infrastructure under adverse and unpredictable conditions [3].

In the literature, many papers considered the capabilities of DERs such as wind turbines (WTs), diesel generators (DGs), electric vehicle parking lots (EVPs), and energy storage systems (ESSs) to enhance the resilience of distribution systems and local energy communities. In [2], a decarbonized pathway was developed to improve the short-term resilience in local energy communities considering the system and HILP event uncertainties. In the paper, a multi-objective resilience-cost objective function was considered to optimally schedule the energy community including the DERs to reduce the impacts of the HILP events. Mobile electrochemical energy storage units can bridge the gap between economically optimal locations during normal operations and areas needing backup during disasters. Ref. [4] proposed an optimization model to invest in and relocate these units dynamically, forming microgrids, and mitigating potential load shedding during disasters using a progressive hedging algorithm due to the complexity of the model. Ref. [5] assessed the impact of the penetration level of DERs in an energy community on grid resilience and offers strategies to manage DER penetration like DGs, WTs, ESSs, and EVPs to enhance resilience while meeting economic objectives. The paper has ignored the impact of the effective load-carrying capability (ELCC) of DERs on grid resilience. The assessment of the power system vulnerabilities to various natural disasters using resilience metrics, employing a mesh-structured view at the transmission level to model the impact of different disasters is presented in [6]. Although the paper modelled the DERs in the system, the ELCC of DERs has been ignored.

A proactive operation scheme for improving distribution system resiliency against natural hazards is proposed in [7]. The paper used a deep neural network engine to identify the vulnerable branches and predict their failure during the windstorm. An optimal resilient operation of the smart distribution systems considering DERs is investigated in [8] using a hybrid stochastic approach to handle the uncertainties. Ref. [9] proposed a stochastic multi-period mixed-integer linear programming model to determine where to underground new distribution lines and how to arrange mobile generators to serve critical loads during extreme events.

Traditional electricity networks rely on conventional assets like transformers but fail to quantify the contribution of ESS in ensuring network security and resilience. [10] introduced a new methodology, using Monte Carlo simulations, to assess the ELCC of an energy storage plant, revealing factors influencing its security contribution such as outage

This work was funded in part by the Eversource project entitled *"A Pathway to Enhance Grid Resilience: Zero-Carbon Energy Communities with DER-based ELCC Quantification"* (PI: Wang).

A. Younesi and Z. Wang are with the Electrical & Computer Engineering Department at the University of Connecticut, Storrs, CT, USA 06268 (e-mails: {abdollah.younesi, zongjie.wang}@uconn.edu). Corresponding author: Zongjie Wang.

T. M. Hansen is with the Electrical Engineering and Computer Science Department, South Dakota State University, Brookings, SD 57007.

frequency, demand shape, and islanding capability. This approach highlights the need for advanced network standards to fairly integrate ESS solutions, enabling fair competition between network and non-network assets for ensuring security in electricity distribution. However, the paper has ignored the resilience metrics and the impact of integrating the ELCC and resilience assessment. Pennsylvania-New Jersey-Maryland (PJM) interconnection is addressing this challenge by enhancing resilience across various aspects like operations, infrastructure, and security. [11] outlines PJM's strategy to assess and manage the impact of high renewable penetration on grid resilience, emphasizing preparation and market-driven approaches for improvement. Although the paper indicated the importance of DER-based ELCC, in the formulations it has ignored the integration of ELCC into the general presented approach.

Based on the aforementioned literature review and the authors' comprehensive understanding, it is evident that DER-based ELCC holds the potential to enhance the resilience of active distribution systems against HILP events. This critical aspect, however, has not been adequately addressed in existing resilience assessment and enhancement methodologies. To address this gap, this paper proposes a stochastic two-stage scheduling approach to reinforce ADN resilience, particularly in systems with high DER penetration. In the proposed method, first, a mesh-view structure is employed to establish interconnections between system components and HILP event locations, which is crucial for assessing post-event damages. In the next step, the ELCC of DERs is quantified and incorporated into our formulations to understand its effect on system resilience. A distinctive feature of our methodology is its carbon-aware approach, which includes constraints on carbon emissions during the generation scheduling process. The framework is validated via a modified IEEE-33 bus standard test case, with results confirming the positive impact of DER-based ELCC on grid resilience. In summary, the main contributions of this paper are as follows:

- Integration of ELCC of DERs into the ADN resilience enhancement method;
- Developing pollution constraints to limit the amount of carbon emissions during the resilience enhancement process;
- Characterizing uncertainties in renewable generation, market prices, and event characteristics (including location, type, and severity level) to make the results more realistic.

This paper is structured as follows: Section II provides a brief overview of the microgrid's cost-effective scheduling technique and the adaptations made to include a detailed ELCC integration. The analysis of simulation case studies conducted on an IEEE 33-bus test system is presented in Section III. Section IV summarizes the findings of this study.

II. Methodology

In this section, first, the general two-stage scheduling method is discussed in Section II-A. Then, in Section II-B, the resilience objective function is formulated to be integrated into the conventional cost objective function. Sections II-C and II-D formulate the ELCC and carbon emission constraints, which will be integrated into the general two-stage scheduling method through the system constraints.

A. The modified ELCC-emission-oriented stochastic two-stage scheduling method

This paper utilizes a stochastic two-stage scheduling method, modifying the objective function to accommodate economic-resilient metrics. For an extensive mathematical formulation of the proposed approach, please refer to [5], [12]. In this paper, the ELCC and carbon emission are quantified and integrated into the proposed two-stage scheduling method. The proposed cost function consists of economic (f_1) and resilience metrics (f_2). Then the constraints are modified in this paper by adding ELCC and carbon emission terms under the impact of a HILP event. The economic objective function consists of costs of day-ahead (or H&N) and real-time (or W&S) variables (see [5]) as follows:

$$f_1 = C_{H\&N} + C_{W\&S}. \tag{1}$$

In the following section, the resilience metrics are mathematically formulated to calculate the resilience objective function.

B. Quantifying resilience metric

This study examines four metrics to assess the resilience of ADNs: the ADN withstand ability quantified through the restoration index (RI) and fragility index (FI), and technical metrics including voltage deviation index (VDI), and lost energy index (LEI). FI and RI gauge the system's capacity to endure and restore after an event, utilizing the ADN performance curve. VDI and LEI assess ADN quality during the event via optimal power flow computations [5]. Fig. 1 exhibits the Performance Curve (PC) of an ADN during a HILP event [3], which is based on the supplied load percentage.

Based on Fig. 1, the FI is calculated as follows:

$$FI \approx \sum_{\omega=1}^{N_\Gamma} \nu_\omega \left[\frac{(PC_{p,\omega} - PC_{pe,\omega})\,(t_{pe,\omega} - t_{d,\omega})}{2PC_{p,\omega}(t_{pe,\omega} - t_{d,\omega})} \right], \tag{2}$$

where Γ is the set of scenarios, N_Γ is the number of scenarios, ν_ω is the probability of each scenario assuming $\omega \in \Gamma$. Using the PC diagram shown in Fig.1 and similar to (2), the RI index is approximated by (3).

$$\begin{aligned} RI \approx \sum_{\omega=1}^{N_\Gamma} \nu_\omega \Bigg[& \frac{(PC_{p,\omega} - PC_{pr,\omega})(t_{irs,\omega} - t_{rs,\omega})}{(PC_{p,\omega} - PC_{pe,\omega})(t_{ire,\omega} - t_{rs,\omega})} \\ & + \frac{(PC_{pr,\omega} - PC_{pe,\omega})(t_{re,\omega} - t_{rs,\omega})}{2(PC_{p,\omega} - PC_{pe,\omega})(t_{ire,\omega} - t_{rs,\omega})} \\ & + \frac{(PC_{p,\omega} - PC_{pr,\omega})(t_{ire,\omega} - t_{irs,\omega})}{2(PC_{p,\omega} - PC_{pe,\omega})(t_{ire,\omega} - t_{rs,\omega})} \Bigg], \end{aligned} \tag{3}$$

The *VDI* and *LEI* metrics indicate the performance of the ADN operation during emergencies following a HILP event,

calculated using optimal power flow (OPF). The *VDI* metric is computed as follows:

$$VDI = \sum_{n=1}^{N_{bus}} \left\{ \sum_{\omega=1}^{N_\Gamma} \nu_\omega \left[\sum_{t=1}^{N_T} \left(|V_{n\omega}^\star| - |V_{nt\omega}| \right) \right] \right\}, \quad (4)$$

where $V_n^\star$ is the scheduled voltage of bus n, $V_{nt\omega}$ is the real-time voltage of bus n at time t and scenario ω, and N_T is the total number of time periods. Similarly, the LEI index is determined based on the lost load as follows:

$$LEI = \sum_{n=1}^{N_{bus}} \left\{ \sum_{\omega=1}^{N_\Gamma} \nu_\omega \left[\sum_{t=1}^{N_T} \left(\frac{P_{nt\omega}^{shed} \Delta t}{p_{nt\omega}^{l} T} \right) \right] \right\}, \quad (5)$$

where Δt is the time interval duration (in this paper $\Delta t = 1$ hour) and $p_{nt\omega}^{l}$ is the real-time load at bus n, time t, and scenario ω. It should be noted that all individual resilience metrics are unitless and for a more resilient system, they should be near zero, therefore, a sum function is used in this paper to map the resilience metrics into the overall ADN resilience score as follows:

$$f_2 = \Re = FI + REI + VDI + LEI. \quad (6)$$

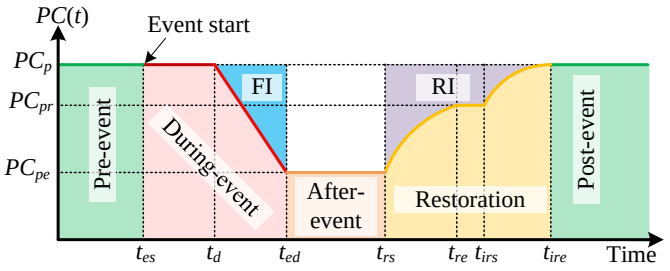

Fig. 1. The ADN performance curve associated with a natural HILP event.

Based on the area depicted for the FI index in Fig. 1, it can be approximately calculated using (2) (please see [5] for more details). It is important to highlight that the system operator possesses the flexibility to allocate distinct weight factors to individual resilience metrics according to their planning priorities. Through the adjustment of these weight factors, the operator can assign varying levels of significance to particular resilience metrics, allowing for customization of the overall resilience index to correspond with the specific goals and requirements of the ADN.

C. Quantifying the ELCC of DERs

The escalating integration of renewable and dispatchable DERs in contemporary ADNs has elevated the significance of DER-based ELCC for ADN operators and operators. DERs' capacity credit holds the potential to swiftly restore ADNs post extreme events and ensure their resilient operation. DER-based ELCC evaluates the capacity value of DER sources, quantifying additional load supply without compromising reliability [13]. This metric relies on reliability measurements like loss of load probability (LOLP) and loss of load expectation (LOLE). The method used for calculating ELCC based on LOLE is depicted in Fig. 2.

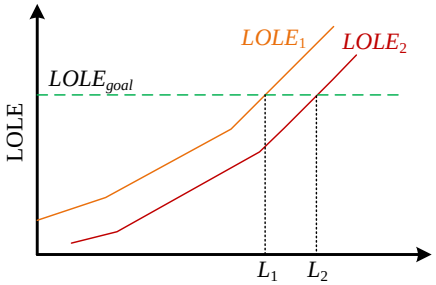

Fig. 2. The reliability after reducing DER units (or increasing load).

As mentioned above, the LOLE is used to calculate the ELCC of the DERs. The LOLE is a well-known reliability index, which is calculated based on the LOLP in both the H&N and W&S stages. In this paper, the LOLP index with some minor modifications (see [5]) is calculated in both stages (i.e., H&N and W&S) using (7) and (8), namely $LOLP^{H\&N}$ and $lolp^{W\&S}$, respectively.

$$LOLP^{H\&N} = \frac{1}{N_T} \sum_{t=t_0}^{N_T} \zeta_t, \quad (7)$$

$$lolp^{W\&S} = \frac{1}{N_\Gamma} \sum_{\omega=1}^{N_\Gamma} \nu_\omega P_{e,\omega} \frac{1}{N_T} \sum_{t=t_0}^{N_T} \zeta_{t\omega}, \quad (8)$$

where $\zeta_{t\omega}$ is a binary variable and is 1 if at time t in the scenario ω the lost load becomes greater than zero (otherwise it is 0), and $P_{e,\omega}$ is the probability of event occurrence. The LOLE index is defined in time periods (e.g. minutes, hours, and days). In this paper, LOLE is defined as follows:

$$LOLE^{H\&N} = LOLP^{H\&N} \times 24 \times 60 \quad \text{minutes/day}. \quad (9)$$

$$lole^{W\&S} = lolp^{W\&S} \times 24 \times 60 \quad \text{minutes/day}. \quad (10)$$

According to Fig. 2, the ELCC is calculated by (11) and based on the flowchart given in Algorithm 1.

$$ELCC_{\%}^{DER} = \left(\frac{L_2 - L_1}{\text{Load}_{\text{total}}} \right) \times 100. \quad (11)$$

Finally, two new inequality constraints are added to the general two-stage scheduling model, as presented in (12) and (13) for the *H&N* and *W&S* stages, respectively. Let $\underline{ELCC}$ and $\overline{ELCC}$ be the minimum and maximum limits of ELCC, respectively.

$$\underline{ELCC} \leq ELCC^{H\&N} \leq \overline{ELCC} \quad (12)$$

$$\underline{ELCC} \leq elcc^{W\&S} \leq \overline{ELCC} \quad (13)$$

D. Quantifying the carbon emission (CE) constraints

Governments shoulder the responsibility of combatting global warming by reducing atmospheric carbon levels, a pivotal approach in addressing climate change. Consequently, the energy sector is pivoting towards net-zero carbon frameworks. This study imposes limitations on carbon-injected energy from sources like DGs and the main grid, aligning with carbon emission considerations. These constraints influence both the stages as follows:

$$CE_t^{H\&N,up} = P_t^{H\&N,b} CI_t^{up}, \quad (14)$$

$$0 \leq CE_t^{H\&N,up} \leq \overline{CE}_t^{up}, \tag{15}$$

$$CE_t^{H\&N,G} = \sum_{n=1}^{N_{bus}} P_{nt}^G CI_{nt}^G, \tag{16}$$

$$0 \leq CE_t^{H\&N,G} \leq \overline{CE}_t^{G}, \tag{17}$$

where $CE_t^{H\&N,up}$ is the carbon emission of the upstream network, $P_t^{H\&N,b}$ is purchased power from the upstream network, CI_t^{up} is the main grid carbon intensity in g/kW, $CE_t^{H\&N,G}$ is the carbon emission of DG units, P_{nt}^G is the generated power of DG at bus n at time t, and CI_{nt}^G is the carbon intensity of DG units in location n at time t. Similarly in the *W&S* stage, the CE constraints are as follows:

$$ce_{t\omega}^{W\&S,up} = p_{t\omega}^{W\&S,b} CI_t^{up}. \tag{18}$$

$$0 \leq ce_{t\omega}^{W\&S,up} \leq \overline{CE}_t^{up}. \tag{19}$$

$$ce_{t\omega}^{W\&S,G} = \sum_{\omega=1}^{N_\Gamma} \nu_\omega \sum_{n=1}^{N_{bus}} p_{nt\omega}^G CI_{nt}^G. \tag{20}$$

$$0 \leq ce_{t\omega}^{W\&S,G} \leq \overline{CE}_t^{G}. \tag{21}$$

Notably, in (14)–(21), the uppercase and lowercase variables are *H&N* and *W&S* stage constraints, respectively.

Algorithm 1 ELCC Calculation Algorithm

input data.
u = 1.
Run ADN Optimal power flow (OPF).
Calculate the $LOLE_u$ index.
Fix the imported power from the main grid equal to the scheduled value from OPF.
repeat:
  u = u+1.
  Gradually increase the ADN load by 1%.
  Run ADN OPF.
  Calculate the $LOLE_u$ using (9) and (10).
  if $LOLE$ remained fixed break the loop.
Calculate the ELCC based on the additional load using (11).

III. Simulation Results and Discussions

A. Test system

The test system used in this paper consists of 33 buses, 33 lines, 5 DGs, 4 ESSs, 4 EVPs, and 4 WTs. The technical data of the system and its components can be found in [3]. The allocation of the DG units is as shown in Fig. 3 [3]. The mesh-view structure [5] is used to calculate the correlation of the system components and event location to assess the system damages following a HILP event. In this paper, it is assumed that the DG carbon emission is fixed at 190 g/kWh throughout the 24 hours of the day and the grid carbon intensity data is collected from the official carbon intensity API for Great Britain developed by National Grid (available at https://carbonintensity.org.uk/)

TABLE I
Comparison of Economic-Resilience-Emission Indices in Different Case Studies.

	Case I	Case II	Case III
Economic index	16317.0045	16369.6196	17582.3011
Resilience index	1.4159	1.2123	1.0679
Carbon emission index [tons]	1.0115	0.8950	0.7866

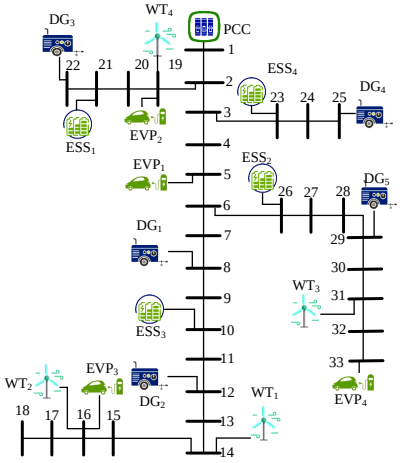

Fig. 3. The standard IEEE-33 bus test system [3].

B. Results

To evaluate the effects of incorporating ELCC constraints into the ADN's two-stage multi-objective method, three case studies have been conducted. Case I excludes ELCC constraints, while Case II applies them with limits of 25% in normal operations and 10% post-HILP events. Case III sets ELCC constraints at 30% for normal operations and 1% for emergencies after HILP events. Essentially, in Cases II and III, DERs have increased flexibility compared to Case I for contributing surplus power during emergencies to boost resilience. With uncertain parameters like market price, event severity and location, and wind turbine generation, 100 scenarios were initially generated based on a uniform probability distribution function, later reduced to 10 for computational efficiency. ELCC impacts on economic, resilience, and emission indices are detailed in Table I.

Table I shows that higher ELCC limits in the ADN lead to increased operating costs but lower resilience and emission indices. This is because the ADN, in normal operations, relies less on DGs and WTs, conserving ELCC for emergencies. This results in purchasing more power from the main grid, thus elevating costs. Reduced power generation from DGs consequently lowers carbon emissions. However, utilizing the ELCC capacity of DGs and WTs during emergencies, as indicated in Table I, improves ADN resilience.

The total carbon emission of the ADN (DGs and main grid) is shown in Fig.4. It should be noted that the HILP event is supposed to start between hours 5:00 PM to 7:00 PM and end between 3:00 AM to 5:00 AM. According to this figure, the emissions in normal operation in Case III are less compared to Cases I and II. As mentioned before, DGs will reduce their generation in this case to be able to share their power in emergencies. During emergencies (i.e., between hours 5:00 PM to 5:00 AM), the carbon emissions of all cases are approximately the same because in this situation the ADN

is discounted from the main grid. Therefore, the grid emission becomes zero and the emission is related to the DGs, which are the same for all cases. Furthermore, to investigate the impact of ELCC on the economic aspect of ADN (i.e., revenue/lost load cost), Scenario 4 has been selected and the revenue and lost load cost of the ADN are shown in Fig. 5 in this scenario.

It can be seen from Fig. 5(a) that considering ELCC has

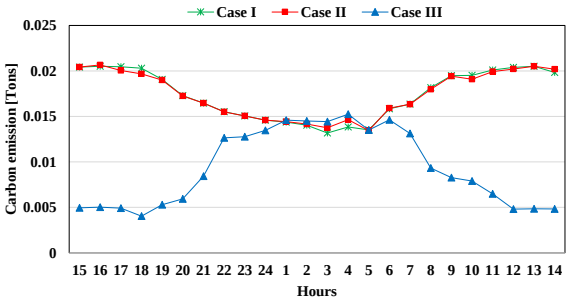

Fig. 4. The carbon emission of the ADN in different case studies.

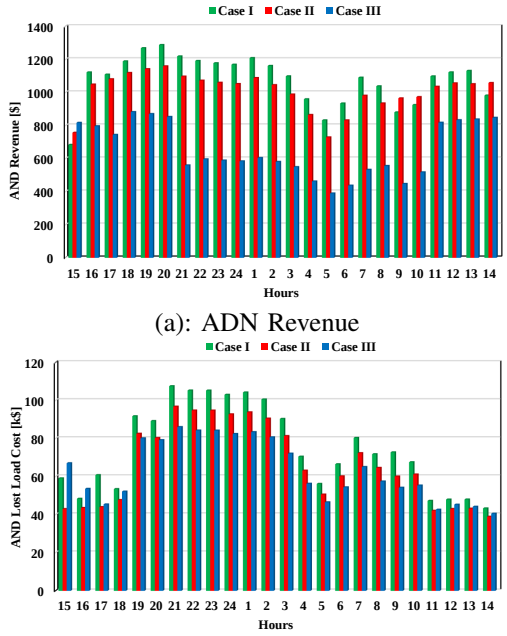

Fig. 5. The economic analysis (revenue/cost) of ADN in different case studies.

decreased the revenue of the ADN. In contrast, Fig. 5(b), shows that the lost load cost of the ADN after a HILP event has been dramatically decreased in Case III compared to Cases I and II. It can be concluded that the reduction in ADN revenue in Case III is spent to reduce the lost load.

IV. Conclusions

The primary objective of this paper is to explore how the effective load-carrying capability (ELCC) of distributed energy resources (DERs) affects the resilience of a decarbonized active distribution network (ADN), particularly under system uncertainties. To achieve this, a stochastic two-stage multi-objective scheduling approach is employed in this paper. The approach uses a mesh-view structure to analyze the correlation between event locations and ADN components, crucial for assessing system damage post high-impact low-probability (HILP) events. This carbon-aware approach integrated the ELCC of DERs to evaluate its impacts on economic, resilience, and emission indices within the system. Simulations on an IEEE-33 bus test system encompass three case studies, each varying in ELCC constraint limitations. The results have demonstrated that while incorporating the ELCC of DERs leads to an increase in operational costs for the ADN, it significantly lowers both resilience and carbon emission metrics. Moreover, although the ELCC inclusion reduces ADN revenue, it substantially cuts lost load costs during emergencies in HILP events, thereby enhancing ADN's overall resilience. Acknowledging the computational challenges inherent in reliability assessments at both ISO and distribution levels, in our future work, the fast-computing tools will be considered to deal with the scalability issues.

References

[1] Y. Li, B. Feng, B. Wang, and S. Sun, "Joint planning of distributed generations and energy storage in active distribution networks: A bi-level programming approach," *Energy*, vol. 245, p. 123226, 2022.

[2] A. Younesi, Z. Wang, P. Siano, and F. Wang, "A pathway to mitigate climate change impacts on energy communities: Decarbonization-based cost-effective grid resilience enhancement," in *2023 IEEE Power & Energy Society General Meeting (PESGM)*, pp. 1–5, IEEE, 2023.

[3] A. Younesi, H. Shayeghi, P. Siano, A. Safari, and H. H. Alhelou, "Enhancing the resilience of operational microgrids through a two-stage scheduling strategy considering the impact of uncertainties," *IEEE Access*, vol. 9, pp. 18454–18464, 2021.

[4] J. Kim and Y. Dvorkin, "Enhancing distribution system resilience with mobile energy storage and microgrids," *IEEE Transactions on Smart Grid*, vol. 10, no. 5, pp. 4996–5006, 2018.

[5] A. Younesi, Z. Wang, S. A. Dorado-Rojas, and P. Mandal, "Quantification of ders penetration level in microgrids: A quest for enhancing short-term power grid resilience," in *2023 IEEE Power & Energy Society General Meeting (PESGM)*, pp. 1–5, IEEE, 2023.

[6] A. Younesi, Z. Wang, and L. Wang, "Investigating the impacts of climate change and natural disasters on the feasibility of power system resilience," in *2022 IEEE Power & Energy Society General Meeting (PESGM)*, pp. 1–5, IEEE, 2022.

[7] M. Mohseni, A. A. Eajal, M. H. Amirioun, A. Al-Durra, and E. El-Saadany, "A learning-based proactive scheme for improving distribution systems resilience against windstorms," *International Journal of Electrical Power & Energy Systems*, vol. 147, p. 108763, 2023.

[8] A. Khodadadi, T. Abedinzadeh, H. Alipour, and J. Pouladi, "Optimal resilient operation of smart distribution network in the presence of renewable energy resources and intelligent parking lots under uncertainties," *International Journal of Electrical Power & Energy Systems*, vol. 147, p. 108814, 2023.

[9] B. Taheri, D. K. Molzahn, and S. Grijalva, "Improving distribution system resilience by undergrounding lines and deploying mobile generators," *Electric Power Systems Research*, vol. 214, p. 108804, 2023.

[10] I. Konstantelos and G. Strbac, "Capacity value of energy storage in distribution networks," *Journal of Energy Storage*, vol. 18, pp. 389–401, 2018.

[11] H. Chen, C. Pilong, P. Rocha-Garrido, D. Frogg, M. Jayachandran, D. Manno, J. Sexauer, C. Callaghan, R. Dropkin, J. Mulhern, *et al.*, "Grid resilience with high renewable penetration: A pjm approach," *IEEE Transactions on Sustainable Energy*, vol. 14, no. 2, pp. 1169–1177, 2022.

[12] A. Gholami, T. Shekari, F. Aminifar, and M. Shahidehpour, "Microgrid scheduling with uncertainty: The quest for resilience," *IEEE Transactions on Smart Grid*, 2016.

[13] L. L. Garver, "Effective load carrying capability of generating units," *IEEE Transactions on Power apparatus and Systems*, no. 8, pp. 910–919, 1966.